

Doctoral (Ph.D.) Thesis

**Preparation and morphological properties of self-assembled
hybrid nanofilms**

Viktória Varga

Supervisor: Dr. Imre Dékány

Professor, member of the Hungarian Academy of Sciences

Chemistry Doctoral School

University of Szeged, Department of Physical Chemistry and Materials Sciences

Szeged

2015

Introduction and aims of the Thesis

Colloids exist in the nanometer range, have at least one dimension and possess variable morphology. Nanoparticles or quantum dots (0D) are nanometric in all three directions and the diameter of wires, rods and tubes (1D) is also in the nanometer scale. The thickness of ultrathin layers and coatings (2D) is also in the nanometer range. On an industrial level, there is a demand for the immobilization of self-assembled structures: nanofilms because in this way portable devices may be obtained that have a large surface. For the aims of this doctoral thesis, the most simple and cost-effective self-assembled layer-by-layer (LbL) film preparation method has been chosen for the synthesis of thin layers from colloids with different sizes and shapes and to examine the possible applications of these layers.

Due to its simplicity, universality and effectiveness, the LbL method is unique among the thin film techniques. As the LbL method is economical in its use of substance, a further advantage of this technique is that it is environmental friendly. By controlling the preparation conditions such as ionic strength, pH, immersion time and cycle number, the layer thickness of the hybrids are reproducible and practically adjustable. One of the richest groups within the LbL layers is the group of polyelectrolyte multilayers (PEM). This group is studied in detail by researchers. Nanoparticles, as film composing components, were first applied in the end of the nineteen-hundreds. The combination of functional materials such as pigments, proteins and DNA together with nanoparticles in thin films holds huge potentials. The production of sensors, electronic and magnetic devices of the future cannot be imagined without LbL technology. The number of publications containing the keyword: layer-by-layer is increasing even today. Every year more than 1200 articles are published in this topic. However, many questions stay open as it is non-equilibrium process. Most of the literature concentrates on the application of this technology without taking into account the electrostatic interactions and secondary binding. Therefore the study of their nearly quantitative effect on the formation of layers, thickness and morphology is essential.

As charge is an important feature in film preparation, the Thesis aims to determine the available amount of the charge of nanoparticles (NPs) as applied in film preparation to explain the charge properties of film composing materials. Using titration method with an oppositely charged surfactant, the specific charge has been determined in a particle charge detector (PCD). The obtained charge values have been compared to the theoretical or known ion exchange capacity values. These values have been calculated from the chemical structure. The thesis makes an attempt to characterize the role of particle charges in film formation and

morphology. Quantitative characteristics of amount and charge on support have been determined from the particle specific charge and the initial concentration data.

To understand film formation mechanisms from the change in absorbance, or layer thickness, with the bilayer number ($n\#$), partially from the type of functions: linear, exponential or second quadrant fitted to the curves and from the slope of linear range i.e. the film building constant (K_{LbL}).

During my doctoral work nanohybrid layers with different charge was prepared to form sensor or reactive surfaces.

The protein-nanoparticle interaction immobilized has been studied in the form of film through a bionano conjugate. This has been constructed by a lysozyme-Au ultrathin nanofilm. In this Thesis, both the role of protein in the change of the plasmonic properties of NPs and the role of NPs in the conformation of protein have been discussed. The LYZ/Au thin layer has been tested as a potential vapour sensor.

An important parameter of self-assembled hybrid layers is their thickness. This has been determined by different methods.

Atomic force measurements (AFM) have been devised to perform a more detailed study of the nanoscale study of thin layers. Through this study, morphological and surface roughness data may be obtained to confirm the results and AFM has also been applied to determine layer thickness.

Materials and Methods

The so-called co-precipitation method was applied to prepare 2:1 Mg-Al layered double hydroxide with NaOH (0,4 M) and Aluminium-nitrate (0,1 M) and Magnesium-nitrate (0,2 M) as precursor and sodium-nitrate (0,1 M).

Polystyrene sulfate (PSS), synthetic Na-hectorite and SiO₂ sol was applied as binding material to immobilize the LDH on the glass surface. The support was Menzel Superfrost glass slide in every case, precisely cleaned prior to use.

To synthesize Prussian blue (PB) dispersions H₂O₂ solution was used apart from the FeCl₂·4H₂O, FeCl₃·6H₂O and K₃[Fe(CN)₆] salts. The polymers to stabilize the dispersion were the followings: poly(vinyl alcohol) (PVA), poly(vinyl-pyrrolidone) (PVP), poly(allylamine hydrochloride) (PAH), poly(diallyldimethylammonium hydrochloride) (PDDA), polyethylene imine (PEI) and PSS. Interdigitated microsensor electrodes (IME)

were used to sensor measurements and the PB layers were immobilized by various methods on their surface.

Na-citrate was used to reduce and stabilize the initial HAuCl₄ solution during the formation of gold colloids (nanoparticles).

The particle size and electrokinetic potential of LDH suspension, Au and Prussian blue (PB) sols were measured by a Zetasizer NanoZs type Malvern apparatus operating using a 632 nm wavelength He-Ne light source. The ζ -potential determinations were performed in a U-shaped capillary sample holder.

The streaming potential of particles can be determined in a so-called particle size detector, Mütek PCD02 type instrument. The unknown specific charge of colloid was determined with the aid of an anionic or cationic (surfactant) with high purity analogue to the volume titration based on the following equation:

$$q_1 = \frac{V_2 \cdot 0.01 \cdot c_2 \cdot q_2}{c_1 \cdot V_1 \cdot M_1}$$

The streaming potential (Ψ) depends on the volume of both participant, where V_1 is the volume in the detector, V_2 is the consumption value. The concentrations of solution/sol/suspension c_1 is in mol/dm³, while c_2 is given in w/V%, the q is in mmol/g with the molar mass (M) of the surfactant in the equation. The charge of dispersions and solutions were determined at the following pH: the silica sol at pH = 7.8, the AuNPs and the lysozyme solution at pH = 6.2. No further salt was added to the dispersion to minimize the effect of the ionic strength. The specific charge data determined by charge titration are summarized in Table 1 [1,2,6,7].

Table 1: Specific charge of different colloids

Material	specific charge (mmol/g)
PSS	-4.75
LDH	0.008
hectorite	-0.5
SiO ₂ sol	-0.3
Au	-0.015
lysozyme	0.08
PB	-0.06
PAH	11.3

Uvikon 930 type Kontron Instrument spectrophotometer was used to characterize the light absorption properties of nanofilms and its components.

The determination of N₂ adsorption isotherms and calculation of specific surface was performed in a Gemini 2375 type automat of Micrometetics instrument at 77 K.

The thermoanalytic measurements were performed by a Derivatograph Q-1500-D instrument (MOM, Hungary) or a Mettler Toledo TGA/SDTA 851e type apparatus.

The X-ray diffraction (XRD) measurements were carried out in a Philips PW 1820 generator-fixed goniometer applying $\lambda = 0.154$ nm wavelength CuK α radiation (40 kV, 30 mA).

The change in protein conformation was studied in a Biorad FTS60A ATR FT-IR spectrophotometer.

The electron microscopy analysis were performed in a Philips CM-10 type transmission electron microscope operating at 100 kV in the Pathology Institute of the Faculty of Medicine of the University of Szeged.

The SEM images were obtained by a FEI Helios Nanolab 600 Dualbeam (FIB-SEM) and a Hicachi S-4700 production field-emission cathode operating at the Department of Applied and Environmental Sciences.

The morphology of the prepared films were characterized by an AFM Nanoscope III. type Digital Instruments scanner. A Veeco Nanoprobe Tips RTESP model silicon tip was used (125 μ m length, 300 kHz frequency and 40 N/m spring constant) during the AFM experiments. The surface roughness (RMS) values were determined by the equation bellow with the V512r5 AFM software which means the average deviation from the average height at a given area:

$$RMS = \sqrt{\frac{\sum_{i=1}^N (Z_i - Z_{aver.})^2}{N}},$$

where Z_i is the of height of the point i , $Z_{aver.}$ is the average height and N is the number of points.

Interdigitated microsensor electrodes (IME) were used to test the sensor properties. The conductivity and resistance were analyzed by a Keithly 2400 series Source meter in the 0.1-2 V direct current range. The limit of detection (LOD) values were determined by the following equation:

$$x_{LOD} = 2x_C = \frac{2t s_y}{n t^2 s_y^2 - D r^2} \left(t s_y \sum x_i - \sqrt{\frac{D^2 r^2}{k} + D r^2 \sum x_i^2 - n \frac{D}{k} t^2 s_y^2 - D t^2 s_y^2} \right),$$

where s_y is the measured signal (current in mV), x_i is the concentration, x_C is the concentration which is larger than the uncertainty, t is the student t-function, n is the number of measured points, D is the determinant, r is the sensitivity, k is the number of parallel measurements.

The build-up of thin films and vapour adsorption properties was followed by a Stanford Research System 200 quartz crystal microbalance (QCM) by using a 5 MHz frequency crystal in static mode. The relation between the measured frequency and the adsorbed mass on the quartz crystal is expressed by the Sauerbrey equation: $\Delta F = -C_f \cdot \Delta m$, where ΔF is the frequency difference between the pure crystal and the adsorbed material, C_f is the sensitivity factor, which is $56.6 \text{ Hz} \cdot \text{cm}^2/\text{mg}$ at room temperature, hence the adsorbed mass (Δm) was obtained in mg/cm^2 .

The surface plasmon resonance spectroscopy (SPR) measurements was used to follow film build-up in a gold covered glass support in a Oriel-goniometer supported home-made system (SPRgoldTM support, Gentel Biosciences).

Film preparation with the LbL method

The glass slide was cleaned and dried prior to film preparation. The surface of glass at neutral and alkaline pH is negatively charged hence positively charged particles can attach and form film due to the electrostatic attraction. As a consequence the surface charge was reversed which facilitated the formation of a subsequent negatively charged layer on top of it. Washing with distilled water was applied between the immersion cycles to remove the excess amount of weakly bound particles. The LbL method to prepare LYZ/Au nanofilm is illustrated in Fig. 1.

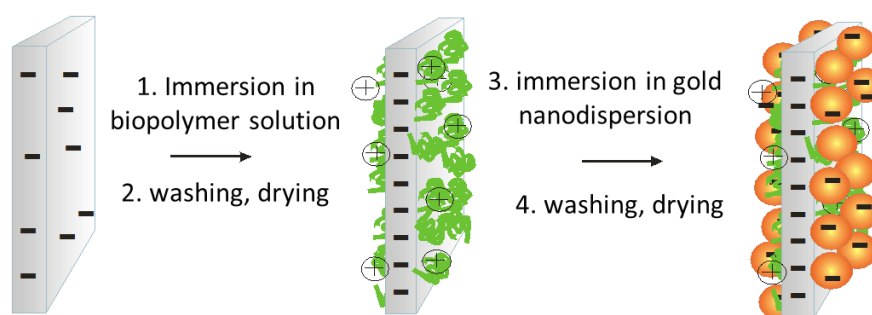


Fig. 1a: Nanofilm preparation with a biopolymer/nanoparticle dispersion interaction (one bilayer)

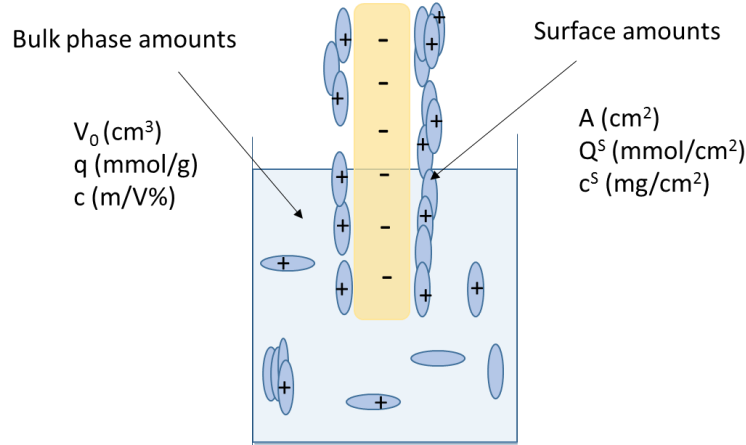


Fig. 1b: Volume (V_0), concentration (c_0) of the bulk phase and the equivalent concentration of charged particle (q)

Surface concentrations (c^S in mg/cm²) of the nanohybrid layer were determined from the calibration of light absorbance of homogenous suspension. The approximate film thickness was calculated from the known c^S and density. The surface mass/initial mass ($c_0 - m/V\%$) ratio ($w^S = m^S/m_0$) was calculated from the deposited surface concentration which means the amount inserted into the layers relative to the total applied amount. To determine the charges present in the liquid phase and on the surface the following equations were used and the amounts are indicated in Fig. 1b. The total mass of LDH in the suspension is denoted by m_0 (mg), while the total adsorbed mass (m^S) was estimated by spectrophotometric method and determined more precisely based on QCM, SEM or AFM measurements. The mass ratio incorporated in the layers is:

$$w^S = \frac{m^S}{m_0} = \frac{c^S \cdot A}{c_0 \cdot V_0},$$

where A is the film surface in cm². The surface charge in mmol can be determined from the specific charge and the layer amounts.

$$Q_{measured}^S = m^S \cdot q = c^S \cdot A \cdot q$$

If we suppose charge equivalence, $Q_{PSS}^S = Q_{LDH}^S$. From a layer model supposing the additive volume based on the geometrical data of the polymer chain, lamellae thickness and density the calculated $Q_{PSS/hectorite/SiO_2}^S$ values can be determined. The layers thickness data are $t_{PSS} = 0.42$ nm, $t_{hectorite} = 1$ nm, $t_{SiO_2} = 15.6$ nm supposing monolayer coverage, thus $Q_{theor.}^S = t \cdot A \cdot \rho \cdot q$, which was compared to the experimental data.

Novel scientific results

T.1. The substantial effect of surface charge in the self-assembly of nanohybrid systems

1.a. The interaction of self-assembled nanoparticles (NPs) and polyelectrolytes was studied in aqueous disperse systems. My experiments verified that the specific charge of nanoparticles and polyelectrolytes with various structure and morphology serve quantitative data to the preparation of the self-assembled layers. The thickness and homogeneity of layers can be tuned by choosing the appropriate concentration ratios based on the determined specific charge ratio. The thickness of the films prepared by immersion dipping technique was varied with the number of deposition cycle and type of components in the 10-740 nm range. The charge ratio $Q = m_1 \cdot q_1 / m_2 \cdot q_2$ determined from the concentration and specific charge of the film composing two components calculated by $Q = m_1 \cdot q_1 / m_2 \cdot q_2$ was varied in a wide range, where $Q_{\text{PSS}}/Q_{\text{LDH}} = 300\text{-}500$, $Q_{\text{hectorite}}/Q_{\text{LDH}} = 15\text{-}65$ and $Q_{\text{SiO}_2}/Q_{\text{LDH}} = 10\text{-}40$. At least 50 times excess of binding components is necessary to obtain homogeneous LDH layers confirmed by microscopic methods. Not uniform layers formed in the case of silica sol, while the amount of SiO_2 (0.25, 0.5 and 1 w/V%) was not enough to reach the required charge excess [2,6,7]. The layer thickness data was calculated from the absorbance of the films compared to the initial suspension absorbance and corrected by the density. The obtained thickness values were corrected from the data obtained by QCM, SEM or AFM measurements. The values determined from spectroscopic method exceeds the real values (AFM, SEM) with at least 20 %, while does not take the film porosity into account, thus resulting in higher q and t values.

1.b. Depending on the initial concentration 0.03-0.6 w/V% LDH was built into the layers if negatively charged PSS, hectorite or SiO_2 sol was applied as the oppositely charge material. Based on the estimated amounts it can be stated that the values calculated geometrically based on the monomolecular coverage and from charge equivalence ($Q_{\text{meas.}}^{\text{S}}$) are in good agreement. The PSS overcharge the LDH layer based on the calculated value. The values calculated for layers containing hectorite or silica are some magnitude lower than the measured values, that is smaller amount build into the layers and the coverage is lower than monomolecular.

T.2. Properties of layered double hydroxide nanohybrid layers prepared from different components (polyelectrolyte or particle)

The layers prepared from polymer are significantly thicker (~500-740 nm) relative that of obtained (60-180 nm) for the films containing hectorite or silica [1,2]. The one order of magnitude higher thickness for PSS films is caused by the one magnitude higher specific charge and the flexibility of the polymer chain and the presence of surface loops. In case of hectorite and silica film, however the role of second-bind is dominant. A loose electrostatic double-layer forms on the support after the washing step. To reveal the mechanism of self-assembly the analysis of shape of layer build-up function is essential and the following statement can be settled.

- i) The charge excess applied in the LDH-PSS films resulted in strong layer hydroxide-polyion complex formation at high charge density, causing thick, stable linearly building layers.
- ii) The increase of immersion time from 10 min to 1 hour has no effect on the thickness of the forming layers, since the electrostatic deposition process completed in 10 min, the coverage achieves its maximum value.
- iii) The build-up characteristics of LDH-hectorite hybrid thin layers changes from the first few layers from linear ($n = 4$) to exponential, while the rougher film surface due to the initial island-like formation enables higher adhered amount.
- iv) The thickness of LDH/PSS layers are mainly determined by the initial concentration of LDH dispersion and secondly, the QPSS/QLDH charge ratio, with its decreasing value the thickness decreases linearly.

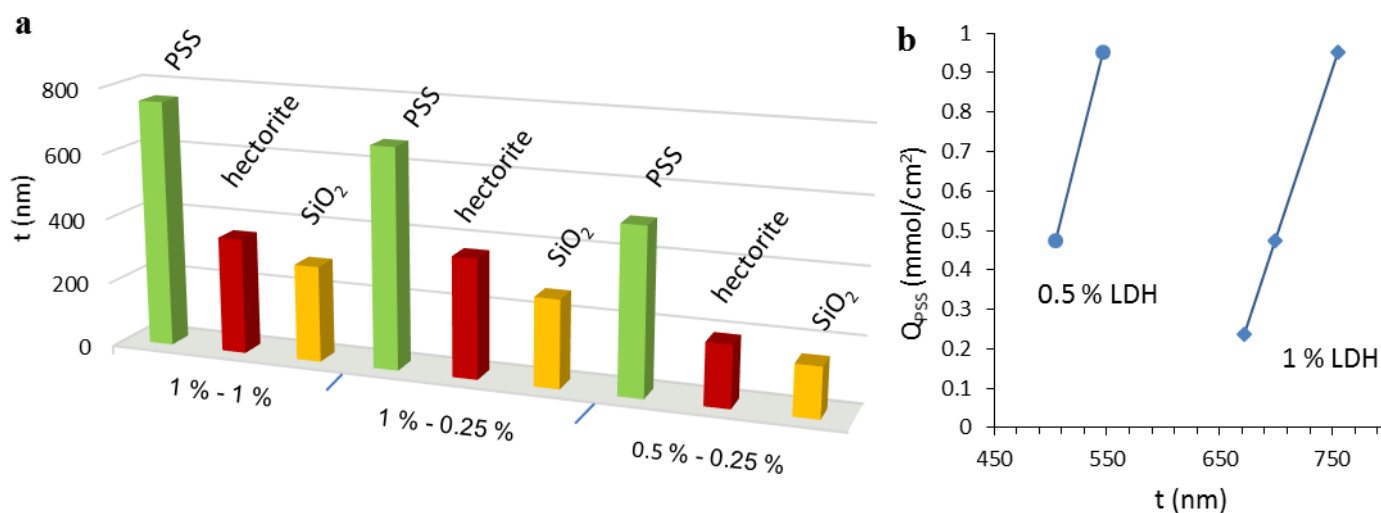


Fig. 2a,b: The thickness of LDH films (a) from different binding component and initial concentration (w/V%) and the change in thickness of LDH/PSS films with surface charge (b)

- v) The thickness in case of SiO₂ films increases along quadratic function with the bilayer number justified by the quadratic correlation between the shell-like coverage on the spherical particles (quadratic correlation between the surface and radius: $lgA \propto 2lgD \cdot \pi \cdot n^{\#}$, where D is the shell thickness).

T.3. *In situ* steric stabilization of prussian blue dispersions and effect of the amount of polymer on the particle size

3.a. Aggregated particles with ~180 nm average size formed in the absence of stabilizing agent in the reaction of Fe³⁺ ion and [Fe(CN)₆]⁴⁻ with H₂O₂ (C_{Fe2+}, C_{Fe3+} = 10 mM, C_{H2O2} = 5 mM). With addition of different types of polyelectrolytes: PAH (d = 42 nm), PDDA (d = 34 nm), PSS (d = 4 nm), PVP (d = 39 nm) and PVA (d = 16 nm), the size was decreased and enhanced stability was gained to achieve appropriate PB sols with high specific surface area with probably higher adsorption capacity for sensor application. Particles with average diameter in the range of 4-40 nm (TEM results) depending on the type and amount of polymer can be prepared.

3. b. By increasing the monomer/Fe²⁺ ratio (between 0-100) in the PVP-stabilized sol the size of the forming K₂Fe[Fe(CN)₆] particles exponentially decreased according to the $\ln y = 0,023d + 3.96$ function from 182 to 18 nm. Its ζ -potential, which is characteristic of the colloid stability increased from -38 mV to -68 mV with the decrease of particle diameter [3]. The phenomenon can be explained by the different rate of the two process determining the particle size: the nucleation and growth. The rate of growth is lower in the presence of polymer, so smaller particles formed sterically stabilized by the polymer chain. The specific surface area at 10:1 monomer/Fe²⁺ composition (3.62 g polymer/g particle) calculated from the diameter ($a^S = 6000/\rho \cdot d$) determined from TEM images was 98 m²/g.

T.4. Utilization of PB-containing thin layer as sensor

The bilayer of 20:1 PVP-PB particle immobilized onto ITE electrodes with 0.25 w/V% PAH polymer proved to be effective in sensing H₂O₂, acetic acid and hydrochloric acid vapour. The PB-modified sensors are effective in redox systems due to the Fe²⁺/Fe³⁺ electron transition. On the other hand, they are pH-sensitive, which makes them applicable in sensing acid vapour. The current signal was measured for PAH/PB sensor at 0.5 mg/cm² surface coverage in the 5-50000 ppm concentration at 0.1-2 V direct current voltage resulted in sensograms with saturation profile in every cases for the vapour of 10-10000 ppm solution [3]. The limit of detection values were determined from the deviation of the measured points from the I – c

calibration curve's initial linear section and proved to be 20 ppm for H₂O₂ for the PAH/PB hybrid film and 22 ppm for acetic acid.

T.5. Formation of lysozyme/Au thin films

The gold sol stabilized by Na-citrate is negatively charged [5] and LYZ is positively charged at pH = 6.2, thus they are capable to form LbL nanohybrid film [6]. The thiol functional groups of the cysteine amino acid coordinated to the Au atoms contributes to the formation of self-assembled nanostructure beyond the electrostatic attraction. It was established that the thickness (30-120 nm) of ultrathin layers linearly changed with the immersion cycle that is the AuNP can compensate the charge of the unfolded protein. It can be stated that the layer thickness increases with 3 times as an effect of increase in immersion time from 10 to 60 min. The layer thickness proved to be about ~ 120 nm for a n = 30 bilayer LYZ/Au determined by both absorbance and AFM measurements which consists of an average 3.1 nm thick Au and a 0.8 nm thick lysozyme layer ($K_{LbL} = 3.9 \text{ nm/n\#}$). The t values indicate that not a well-packed monomolecular layer formed from the AuNPs, the value of K_{LbL} is smaller than the diameter of a particle or a globular protein. However, the thickness of the LYZ layer refers to the thickness of the carbon backbone, implying that the protein is in unfolded state in the LYZ/Au bilayers.

T.6. Plasmonic properties of LYZ/Au thin layers

The change in colour from the originally red-wine gold sol (0.02 w/V%) to blue is explained by the AuNP aggregation as an effect of interaction with lysozyme [5]. The liquid phase experiment of LYZ/Au also proved the aggregation, since the λ_{max} value changed from 530 nm to 620 nm and a new peak evolves at 765 nm which indicated the presence of aggregated anisometric AuNPs at LYZ: Au = 1:20 ratio. The linkage between the particles can be also perceived in the TEM images and the visible absorption spectrum verified the aggregation process. Above $n \geq 5$ bilayer the metallic character of Au can be observed in the form of golden colour and mirror reflecting surface which indicates increasing homogeneity [6]. With increasing layer number around 20 bilayers ($t = 74 \text{ nm}$) the AuNPs compose coherent layers. The surface roughness values also verify the increasing homogeneity with 31.3 nm RMS value for the n = 30 contrary to the RMS = 56 nm value for n = 10.

T.7. Thickness and porosity of LYZ/Au thin films

The thickness of LYZ/Au thin layers was determined from the cross sectional image of the scratched/broken layers determined by SEM and AFM. The results were compared to the values calculated from the absorbance values at 400 nm wavelength and obtained a maximum of $\pm 7\%$ deviation. The differences in thickness values determined from AFM and QCM methods denote film porosity. The QCM assumes bulk phase layers, while the AFM reveals the real, porous cross-section structure. The porosity (ε) can be calculated from the values determined from the two method:

$$\varepsilon = \frac{V_t - V_{QCM}}{V_t} = \frac{t_{AFM} - t_{QCM}}{t_{AFM}}$$

The porosity for a $n = 30$ LYZ/Au bilayer film is 0.4, that is 40 %.

T.8. AFM characterization of LbL layers

The AFM was applied to determine layer thickness and to compare roughness data with mechanism of film buildup beyond the conventional morphology characterization. The LDH/PSS layers displayed the most homogeneous surface among the LDH films with RMS = 125 nm roughness for the 1 w/V% LDH - 0.5 w/V % PSS film. With decreased amount of PSS (1 w/V% - 0.25 w/V%) the roughness increased to 250 nm which is in accordance with the less than optimal charge ratio (50-times, see T.1.). By applying hectorite or SiO₂ binding component, the lamellar characteristic of hectorite can be seen or the separated, island-like presence of spheres and lamella packages in case of LDH/silica films (RMS = 150, 165 nm). Based on the AFM image of hybrid film built from 0.5 w/V% LDH – 0.25 w/V% PSS ($n = 10$) the polyelectrolyte covers the lamellae and a more uniform film forms (RMS = 140 nm), contrary to the 1 w/V% LDH containing films, where the smaller polymer concentration (0.25-0.5 w/V%) cannot hinder the lamella stacking, so assemblies of lamella aggregates with $h = 400$ -500 nm height form [1,4].

The PAH/PB ($n = 10$) and the LYZ/Au ($n = 30$) hybrid layers are relatively homogeneous and smooth with RMS = 24 and 32 nm roughness values. The spherical structure on their surface can be observed; both the PAH and the LYZ sterically stabilize the nanoparticles and cover them with a thin layer. The linearity of the buildup verify the charge compensation between the components.

T.9. The LYZ/Au films as possible vapour adsorption sensors

The LYZ/Au thin film of $n = 30$ bilayers were tested for the first time in sensing vapours with different polarity and functional groups with QCM in a static system. Surface coverage data were calculated from the adsorbed mass (Δm) in the knowledge of surface area (a_m): $\Theta = \Delta m/M \cdot a_m$. Due to the polar characteristic of the film low capacity was measured for toluene, while similar values (1.22; 1.32, 1.45), 20-45 % above the monomolecular coverage, were obtained for water ethanol and acetic acid. Around one magnitude higher (7.72-times) than the monomolecular coverage value was measured for NH_3 [6]. The film porosity explains that the coverage exceeds monomolecular values high activity and the higher vapour tension of ammonia relative to the other tested vapours. If the adsorbed amounts are normalized by the vapour tension values (Θ/p_0) the data calculated for ammonia is not significant, but water caused highest value and then acetic acid, ammonia, ethanol and toluene.

Publications

Papers related to the Thesis published in refereed journals

[1] V. Hornok, A. Erdőhelyi, I. Dékány:
Preparation of ultrathin membranes by layer-by-layer deposition of layered double hydroxide (LDH) and polystyrene sulfonate (PSS).
Colloid and Polymer Sci. 283, 1050-1055 (2005)
IF: **1.263**, times cited: **31**

[2] V. Hornok, A. Erdőhelyi, I. Dékány:
Preparation of ultrathin membranes by layer-by-layer (LBL) deposition of oppositely charged inorganic colloids
Colloid and Polymer Sci. 284, 611-619 (2006)
IF: **1.249**, times cited: **18**

[3] V. Hornok, I. Dékány:
Synthesis and stabilization of Prussian blue nanoparticles and application for sensors.
Journal of Colloid and Interface Sci. 309 (1), 176-182 (2007)
IF: **2.309**, times cited: **32**

[4] T. Aradi, V. Hornok, I. Dékány:
Layered double hydroxides for ultrathin hybrid film preparation using layer-by-layer and spin-coating methods
Colloids and Surfaces A 319 (1-3), 116-121 (2008)
IF: **1.926**, times cited: **18**

[5] A. Majzik, R. Patakfalvi, V. Hornok, I. Dékány:
Growing and Stability of Gold Nanoparticles and their Functionalization by Cysteine
Gold Bulletin 42 (2009) 113-123
IF: **2.324**, times cited: **27**

[6] E. Pál, V. Hornok, D. Sebők, A. Majzik, I. Dékány:
Optical and structural properties of protein/gold hybrid bio-nanofilms prepared by layer-by-layer method
Colloid and Surfaces B 79 (2010) 276-283
IF: **2.780**, times cited: **8**

[7] T. Bujdosó, V. Hornok, I. Dékány:
Thin films of layered double hydroxide and silver and silver-doped polystyrene particles
Applied Clay Science 51 (3) (2011) 241-249
IF: **2.303**, times cited: **1**

$$\sum_{i=1-7} I.F. = 14.154$$

Other papers published in referred journals

8. Á. Patzkó, R. Kun, V. Hornok, T. Engelhardt, N. Schall:

ZnAl-layer double hydroxides as photocatalysts for oxidation of phenol in aqueous solution
Colloids and Surfaces A 265, 64-72 (2005)

IF: **1.499**, times cited: **51**

9. E. Pál, D. Sebők, V. Hornok, I. Dékány:

Structural, optical and adsorption properties of ZnO₂/poly(acrylic acid) hybrid thin porous films prepared by ionic strength controlled layer-by-layer method

Journal of Colloid and Interface Science 332 (2009) 173-182

IF: **3.019**, times cited: **19**

10. E. Pál, V. Hornok, A. Oszkó, I. Dékány:

Hydrothermal synthesis of prism-like and flower-like ZnO and indium-doped ZnO structures

Colloids and Surfaces A 340 (2009) 1-9

IF: **2.780**, times cited: **46**

11. T. Szabó, V. Hornok, RA. Schoonheydt, I. Dékány :

Hybrid Langmuir-Blodgett monolayers of graphite oxide nanosheets

Carbon 58 (2010) 1676-1680

IF: **4.893**, times cited: **18**

12. V. Hornok, T. Bujdosó, J. Toldi, K. Nagy, I. Demeter, C. Fazakas, I. Krizbai, L. Vécsei, I. Dékány:

Preparation and properties of nanoscale containers for biomedical application in drug delivery: preliminary studies with kynurenic acid

Journal of Neural Transmission 119 (2011) 115-121

IF: **2.597**, times cited: **4**

13. E. Csapó, R. Patakfalvi, V. Hornok, L.T. Tóth, Á. Sipos, A. Szalai, M. Csete, I. Dékány:
Effect of pH on stability and plasmonic properties of cysteine-functionalized silver nanoparticle dispersion

Colloids and Surfaces B 98 (2012) 43-49

IF: **3.456**, times cited: **28**

14. G. Bohus, V. Hornok, A. Oszkó, A. Vértes, E. Kuzmann, I. Dékány:

Structural and luminescence properties of Y₂O₃:Eu³⁺ core-shell nanoparticles

Colloids and Surfaces A 405 (2012) 6-13

IF: **2.236**, times cited: **4**

15. E. Pál, V. Hornok, R. Kun, V. Chernyshev, T. Seemann, I. Dékány, M. Busse:

Growth of raspberry-, prism- and flower-like ZnO particles using template-free low-temperature hydrothermal method and their application as humidity sensors

Journal of Nanoparticle Research 14 (2012) 14

IF: **3.287**

16. K. Lázár, T. Belgya, E. Csapó, I. Dékány, V. Hornok, S. Stichleutner:

In-beam Mössbauer-spektroszkópia

Nukleon 5:120 (2012) 7

17. E. Pál, V. Hornok, R. Kun, A. Oszkó, T. Seemann, I. Dékány, M. Busse:

Hydrothermal synthesis and humidity sensing property of ZnO nanostructures and ZnO-In(OH)₃ nanocomposites

Journal of Colloid and Interface Science 378 (2012) 100-109

IF: **3.07**, times cited: **4**

18. L. Körösi, S. Papp, V. Hornok, A. Oszkó, P. Petrik, D. Patkó, R. Horváth, I. Dékány: Titanate nanotube thin films with enhanced thermal stability and high-transparency prepared from additive-free sols

Journal of Solid State Chemistry 192 (2012) 342-350

IF: **2.159**, times cited: **8**

19. A.M. Youssef, T. Bujdosó, V. Hornok, S. Papp, A.E.A. Hakim, I. Dékány: Structural and thermal properties of polystyrene nanocomposites containing hydrophilic and hydrophobic layered double hydroxides

Applied Clay Science 77-78 (2013) 46-51

IF: **2.342**, times cited: **3**

20. A. Majzik, V. Hornok, D. Sebők, T. Bartók, L. Szente, K. Tuza, I. Dékány: Sensitive detection of Aflatoxin B1 molecules on gold SPR chip surface using functionalized gold nanoparticles

Cereal Research Communication 13 (2015) 426-437

IF₂₀₁₄: **0.624**

21. A. Majzik, V. Hornok, N. Varga, R. Tabajdi, I. Dékány:

Functionalized gold nanoparticles for 2-naphthol binding and their fluorescence properties

Colloids and Surfaces A 481 (2015) 244-251

IF₂₀₁₄: **2.752**

Conference presentations

Oral presentations

1. Viktória Hornok, Márta Szekeres, András Erdőhelyi, Imre Dékány:

Ultravékony rétegek előállítása, szerkezete és felületi morfológiájának vizsgálata AFM technikával

4th Hungarian SPM Meeting, Szeged, 21 April 2006

2. Viktória Hornok:

Az atomi erő mikroszkóp kolloidkémiai alkalmazásai

Az élőlényektől az atomokig, vizsgálatok pásztázó mikroszkópokkal

MTA-SZAB Kémiai szakbizottság, Anyagtudományi Munkabizottság, Magyar Tudomány Ünnepe, Szeged, 8 November 2007, MTA SZAB

3. Viktória Hornok, Mária Benkő, Imre Dékány:

Dynamic light scattering for the determination of particle size distribution and z-potential of nanoparticles. Special applications in the 2-20 nm range with Horiba SZ-100

Francelab Scientific Days, 25-27 February 2014, France Institute, Budapest

4. Viktória Varga:

Réteges felépítésű önszerveződő hibrid nanofilmek, szerkezetük és tulajdonságaik

SZAB Kémiai Szakbizottság Anyagtudományi Munkabizottsága „Anyagtudományi Kutatások Szegeden” rendezvénysorozat, 13 May 2014, MTA SZAB, Szeged

5. Viktória Hornok:

Önszerveződő hibrid nanofilmek szerkezete és morfológiai tulajdonságaik – PhD Thesis
SZAB Kémiai Szakbizottság Anyagtudományi Munkabizottsága, MTA SZAB, 20 October
2014, Szeged

6. Viktória Hornok, Edit Csapó, Noémi Varga, Ádám Juhász, Dániel Sebők, Imre Dékány:
Nanokapszulás kompozit rendszerek tervezése: szerkezeti és termodinamikai összefüggések.
Kinurenin Kerekasztal, MTA SZAB, 21 May 2015, Szeged

Poster presentations

1. J. Ménesi, V. Hornok, A. Erdőhelyi, I. Dékány:

Self-assembled layered double hydroxide/polymer composites for gas separation.

8th International Symposium on Interdisciplinary Regional Research (ISIR), 19-21 April 2005,
Szeged, Hungary

2. T. Szabó, I. Konfár, J. Ménesi, V. Hornok, I. Dékány:

Structure and electronic properties of graphite oxide and its polymer composite

European Materials Research Society (E-MRS) 2005 Spring Meeting

31 May – 3 June 2005, Strasbourg, France

3. J. Ménesi, V. Hornok, A. Erdőhelyi, I. Dékány:

Self-assembled layered double hydroxide/polymer composites and polymer nanofilms: the
effect of salt concentration on the film thickness.

E-MRS Spring Meeting, May 31 – June 3, 2005, Strasbourg, France

4. V. Hornok, É. Sija, I. Dékány:

Synthesis and stabilization of Prussian blue nanoparticles and application for sensors.

20th Conference of the European Colloid and Interface Society 18th European Chemistry at
Interfaces Conference (ECIS-ECIC), 17-22 September 2006, Budapest, Hungary

5. T. Aradi, V. Hornok, I. Dékány:

Layered double hydroxides for ultrathin film preparation using layer-by-layer and spin
coating methods.

20th ECIS, 18th ECIC, 17-22 September 2006, Budapest, Hungary

6. E. Pál, V. Hornok, I. Dékány:

Investigation of fluorescent CdS, ZnO, and doped ZnO nanolayers prepared by LbL
immersion method

20th ECIS, 18th ECIC, 17-22 September 2006, Budapest, Hungary

7. A. Majzik, R. Patakfalvi, V. Hornok, I. Dékány:

Gold nanoparticle growing and stability, their functionalization by cysteine

23rd ECIS, 6-11 September 2009, Antalya, Turkey

8. T. Szabó, R. Schoonheydt, V. Hornok, I. Dékány:

Preparation of ordered graphene nanolayers by Langmuir-Blodgett deposition of exfoliated
graphite oxide

23rd ECIS, 6-11 September 2009, Antalya, Turkey

9. V. Hornok, I. Dékány:
Preparation and characterization of lysozyme nanofilms prepared by LbL method.
23rd ECIS, 6-11 September 2009, Antalya, Turkey
10. E. Csapó, A. Majzik, V. Hornok, Sz. Papp, N. Fejős, L. Fülöp, B. Penke, I. Dékány:
Characterization of amino acid- and peptide-conjugated gold and silver nanoparticles
24th ECIS, 5-10 September 2010, Prague, Czech Republic
11. E. Csapó, V. Hornok, Á. Juhász, M. Csete, I. Dékány:
Characterization of amino acid- and peptide conjugated gold and silver nanoparticles
Euronanoforum 30 May – 1 June 2011, Budapest
12. Á. Sipos, A. Szalai, E. Csapó, R. Patakfalvi, V. Hornok, M. Csete, I. Dékány:
Numerical investigation of the plasmonic properties of bare and cysteine-functionalized silver nanoparticles aggregates
Euronanoforum 30 May – 1 June 2011, Budapest
13. E. Csapó, V. Hornok, A. Sipos, A. Szalai, M. Csete, D. Sebők, I. Dékány:
Plasmonic properties of biofunctionalized gold/silver nanoparticles at different pH in aqueous dispersion
Biological Surfaces and Interfaces, 26 June – 1 July 2011. SantFeliu de Guixols, Spain
14. V. Hornok, T. Bujdosó, T. Rica, A.A. AbdEl-Hakim, A.M. Youssef, O.R.A. Soliman, I. Dékány:
Stabilization of polymer hybrid nanocomposites using functionalized Zn-Al layer double hydroxides
16th International Symposium on Intercalation Compounds (ISIC), 22-27 May 2011, Seč-Ústupy, Czech Republic
15. T. Szabó, V. Hornok, I. Dékány:
Hybrid Langmuir monolayers of graphene oxide nanosheets/octadecyl-Rhodamine B and their derived graphene films
Carbon 24-29 July 2011 Shanghai, China
16. E. Pál, V. Hornok, R. Kun, T. Seemann, I. Dékány and M. Busse:
Raspberry-, and prism-like ZnO nanoparticles and ZnO-In(OH)₃ nanocomposites prepared by hydrothermal method
25th ECIS, 2-9. September 2011, Berlin, Germany
17. E. Csapó, V. Hornok, D. Sebok, G. Bohus, S. Papp and I. Dékány:
Characterization of biofunctionalized noble metal nanoparticles for biomedical and sensor applications
25th ECIS, 2-9 September 2011 Berlin, Germany
18. E. Pál, V. Hornok, R. Kun, A. Oszkó, I. Dékány. M. Busse:
Hydrothermal synthesis and humidity sensing property of ZnO nanostructures, ZnO-In(OH)₃ and ZnO-In₂O₃ nanocomposites
5th Szeged International Workshop on Advances in Nanoscience (SIWAN) 24-27 October 2012, Szeged, Hungary

19. E. Kuzmann, A. Vértes, G. Bohus, V. Hornok, A. Oszkó, I. Dékány: ^{151}Eu Mössbauer study of luminescent $\text{Y}_2\text{O}_3:\text{Eu}^{3+}$ core-shell nanoparticles
International Conference on the Applications of the Mössbauer Effect (ICAME 2012), Invited talk at the International Conference on the Applications of the Mössbauer Effect (ICAME) 1-7 September 2012, Dalian, China

Patent

I. Ábrahám; T. Aradi; V. Hornok, I. Dékány et al. - Inventor(s)

Flow-through measuring cell for use in charge-compensation measuring device, has integral measuring channel which connects the inlet port and discharge port, and is provided between inner surface of cell house and shearing unit

Patent Number: HU200900422-A1

Patent Assignee: University of Szeged; Unichem Ltd. 2009

Full journal papers, total: 21

Cumulative impact factor, total: 48.868

Independent citations, total: 257

related to the topic of the Theses: 7

related to the topic of the Theses: 14.154

related to the topic of the Theses: 113